

## Opportunities and Difficulties with $5 \times 5$ Distillation Control

Petter Lundström and Sigurd Skogestad\*

Chemical Engineering,  
University of Trondheim, NTH,  
N-7034 Trondheim, Norway

**Abstract** Multivariable  $5 \times 5$  distillation control provides opportunities to improve the control performance as compared to decentralized control. The main advantage is automatic constraint handling which can not be realized by a fixed linear controller, but requires a solution based on on-line optimization, for example, using a Model Predictive Control (MPC) strategy. In this paper this approach is combined with the  $\mathcal{H}_\infty/\mu$  framework in order to get a robust design.

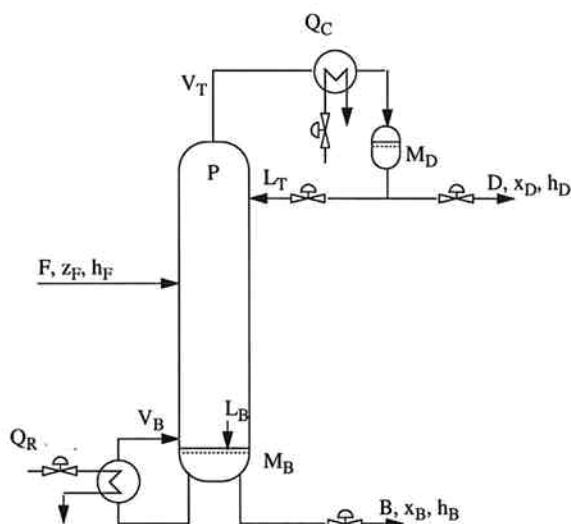


Fig. 1: One-feed two-product distillation column.

### 1 Introduction

A one-feed two-product distillation column, as shown in Fig.1, may be viewed as a  $5 \times 5$  dynamic system. This means that for a fixed design and a given feed the column has 5 (dynamic) degrees of freedom, or in control terms, there are 5 manipulated inputs which may be used to control 5 controlled outputs. The controlled variables (outputs) are the liquid holdup in reboiler and condenser ( $M_B$ ,  $M_D$ , here assumed on a molar basis), pressure in the condenser ( $P_D$ ), composition of light component in the top product (distillate) ( $x_D$ ) and composition of light component in the bottom product (bottoms) ( $x_B$ ). In this paper all controlled outputs are measured, but measurement error is included in the analysis. The manipulated variables (inputs) are the flows of reflux, distillate and bottoms ( $L_T$ ,  $D$  and  $B$ , here assumed on a molar basis), and the heat duty in reboiler and condenser ( $Q_R$ ,  $Q_C$ ). The feed rate ( $F$ ), composition ( $z_F$ ) and energy content (defined in terms of the bub-

ble point pressure of a liquid feed,  $P_F^{sat}$ ) all act as disturbances.

In industry most columns are operated by single-input-single-output (SISO) controllers and manual adjustments. Such a decentralized (multiloop) control structure has the advantage of being easy to retune and to understand. However, fixed pairing of outputs and inputs may limit the performance of the overall system, since the SISO controllers do not utilize information from the other loops. Another disadvantage with decentralized control is that the control structure may have to be reconfigured and retuned if the system hits some constraint.

From a theoretical point of view it is obvious that the 'optimal' controller should use *all* available information (measurements, plant model, expected model uncertainty, expected disturbances, known future set-point changes, known constraints, etc.) to manipulate all 5 inputs in order to keep all 5 outputs at their optimal values ( $5 \times 5$  control) (Skogestad 1989). It is also clear that constraint handling is a very important issue for this 'optimal' control scheme, since, in general, optimality is obtained at some constraint, for example, maximum throughput.

A fundamental difficulty with any optimizing scheme is to define an objective function which yields a mathematically optimal solution in agreement with what is actually desired. Another problem is to obtain sufficiently certain information (measurements, plant model, uncertainty bounds, etc.) to make the optimization worthwhile.

The purpose of this paper is to evaluate the opportunities and difficulties with applying  $5 \times 5$  control to a distillation column. The paper is organized as follows. In section 2 we present a fairly rigorous non-linear  $5 \times 5$  model, which, contrary to most other distillation models, does not assume constant pressure (which would yield a  $4 \times 4$  model). In section 3 we perform a controllability study using a linearized model. We also consider decentralized control which leads to rather poor performance for the example column in question. In section 4 we study the *unconstrained* multivariable problem, using the  $\mathcal{H}_\infty$ -norm to measure control performance. This norm makes it possible to specify desired responses in terms of closed-

\* Author to whom correspondence should be addressed. E-mail: skoge@kjemi.unit.no, Phone: +47-7359-4154, Fax: +47-7359-4080

Feed ( $d$ ):	$F$	=	1.0 [kmol/min]
	$z_F(1)$	=	0.5 [kmol/kmol]
	$P_F^{sat}$	=	0.11 [MPa]
Controlled outputs ( $y$ ):	$x_D(1)$	=	0.99 [kmol/kmol]
	$x_B(1)$	=	0.01 [kmol/kmol]
	$P_D$	=	0.1 [MPa]
	$M_D$	=	32.1 [kmol]
	$M_B$	=	11.0 [kmol]
Manipulated inputs ( $u$ ):	$L_T$	=	2.725 [kmol/min]
	$Q_R$	=	129.09 [MJ/min]
	$Q_C$	=	-129.02 [MJ/min]
	$D$	=	0.5 [kmol/min]
	$B$	=	0.5 [kmol/min]
Key hydraulic parameters:	$\bar{\tau}_L$	$\approx$	2.4 [sec]
	$\sum \tau_L$	$\approx$	93 [sec]
	$K_{2(Top)}$	$\approx$	0.5
	$K_{2(Bot)}$	$\approx$	0.8

loop time constants, allowable steady state offset and acceptable overshoot, and also allows us to address robustness using the structured singular value,  $\mu$  (Doyle 1982). In section 5 we consider model predictive control consider using a state observer based MPC algorithm (Morari et al. 1991). We first attempt to tune the unconstrained MPC controller to mimic the performance of the robust  $\mathcal{H}_\infty/\mu$  controller by using  $\mu$ -analysis and the weights obtained from the  $\mathcal{H}_\infty$ -case. Of course, this may not be done directly as an MPC controller behaves similar to an  $H_2$  controller, which is not quite the same as an  $\mathcal{H}_\infty$ -controller (the norms are somewhat different). When the unconstrained performance has been assessed, we use simulations to evaluate the performance for the constrained case.

## 2 $5 \times 5$ Distillation Model

In this section we briefly present the distillation column which is used as an example process in the rest of the paper. The example column separates a binary mixture into a top and a bottom product of relatively high purity (99%). The column closely matches “column A” studied by Skogestad and Morari (1988), but the model is much more detailed:

1. Pressure is not assumed constant.
2. Vapor holdup is included.
3. Liquid flow rate is computed from the Francis weir formula, including a correlation between vapor flow and froth density (Bennett et al. 1983) such that a change in vapor flow will have an initial effect on the liquid flow (the “ $K_2$ ”- or “ $\lambda$ -effect”, Rademaker et al., 1975).

This yields a model with 3 states (differential equations) per control volume (the molar holdup of each component and the internal energy), resulting in a total of 123 states for our column with 39 stages plus total condenser and reboiler. The nonlinear model

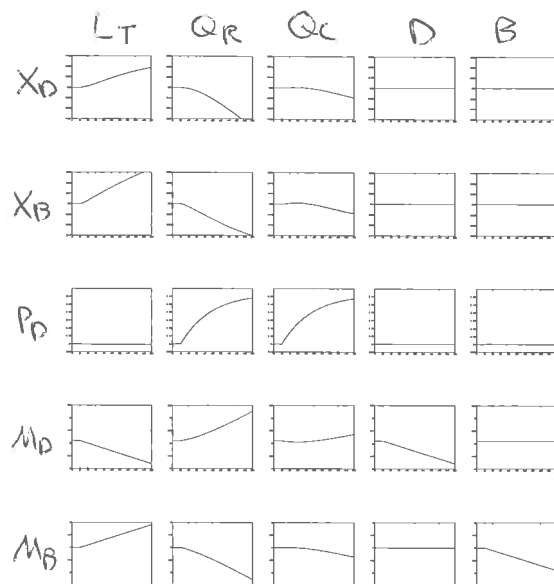


Fig. 2: Open loop step responses showing the effect of the 5 inputs ( $u$ ) on the 5 outputs ( $y$ ). 200 min simulation time.

has been implemented in the equation oriented simulation package SPEEDUP. A UV-flash, with fixed overall composition, internal energy and total volume on each tray, is used for equilibrium computation.

A summary of the column data are given in Table 1. Open-loop time responses are summarized in Figure 2. Note that we assume that the heating and cooling duties are adjusted directly, that is, there is no self-regulation and  $Q_C$  and  $Q_R$  are not affected by changes in pressure and temperature in the column. This may be the case, for example, if heat is provided by condensation, and cooling is provided by boiling. This assumption yields are very long time constant for the open-loop pressure response, and it may be estimated to be about  $(M_L + 4M_V)/F = 74 \text{ min}^1$ .

## 3 Controllability analysis

In this section simple linear tools (e.g., Wolff et al., 1992) are used to assess the controllability properties of the plant, that is, to evaluate any inherent performance limitations. The results from the controllability analysis is also used to specify realistic requirements for control performance and thereby reduce the need for iterative adjustments of the performance requirements, i.e the ‘weights’ used to tune the controller.

<sup>1</sup>This formula is derived from an overall heat balance assuming the temperature change is the same throughout the column. The factor 4 for the vapor holdup is a typical value, and is due to fact that  $c_{PV} > c_{PL}$  and that some energy is needed for evaporation when pressure increases. If we have self-regulation in the condenser, e.g.,  $Q_C = UA(T_{cool} - T_D)$ , then we get  $F + UA/c_{PL}$  in the denominator instead of  $F$ , and the time constant is much smaller, typically about 2 min.

Table 2: Maximum changes for scaling. (Units and order for vectors are given in Table 1.)

Output error:	$y_{max}$	=	[0.01 0.01 0.050 30. 10.]
Setpoints:	$r_{max}$	=	[0.01 0.01 0.025 0.5 0.5]
Inputs:	$u_{max}$	=	[2.7 130 130 0.5 0.5]
Feed disturbances:	$d_{max}$	=	[0.15 0.1 0.025]

**Scaling.** The RGA and the poles and zeros are independent of scaling, but most other measures depend critically on scaling. Therefore, all results and plots in the following are in terms of scaled variables, i.e., all outputs, setpoints, inputs and disturbances are scaled by a given maximum value to stay within  $\pm 1$ . The maximum values used for scaling are summarized in Table 2<sup>2</sup>. For example, the scaled reflux (input) is  $u_1 = \Delta L_T / L_{T,max}$ , where  $L_{T,max}$  is the maximum allowed change in reflux. From Table 2  $L_{T,max} = 2.7$  kmol/min, and since this is equal to the nominal flow, we get that  $u_1 = -1$  corresponds to zero reflux.

**Relative gain array (RGA).** The steady state RGA for the linearized  $5 \times 5$  plant is:

	$L_T$	$Q_R$	$Q_C$	$D$	$B$
$x_D$	36.76	-64.65	28.88	0.00	0.00
$x_B$	-35.72	63.49	-26.76	0.00	0.00
$P_D$	-0.04	2.16	-1.12	0.00	0.00
$M_D$	0.00	0.00	0.00	1.00	0.00
$M_B$	0.00	0.00	0.00	0.00	1.00

The conventional ‘‘LV-configuration’’, which is considered in this paper, corresponds to pairing on the diagonal elements. The first observation from the steady-state RGA is that the 4,4 and 5,5 elements are 1.0 while all other elements in columns 4 and 5 and rows 4 and 5 are zero. Following the conventional pairing rule for decentralized control we should pair on elements close to 1, i.e. use  $D$  to control  $M_D$  and  $B$  to control  $M_B$ .

The second observation is that the 3,3 element is negative. From the results of Grosdidier et al. (1985) we know that a decentralized control scheme with integral action paired on this negative RGA element leads to 1) Overall system unstable, or 2) Pressure loop unstable, or 3) Remaining system unstable if pressure loop fails. In practice, this means that using  $Q_C$  to control  $P_D$  and tuning for a stable pressure loop and a stable overall system leads to instability if the pressure loop fails, e.g. if  $Q_C$  saturates. Thus, one must be very careful to avoid saturation for the pressure control<sup>3</sup>.

Another observation is that there is strong two-way interactions in the upper left  $3 \times 3$  subsystem, while there is no two-way interaction in the rest of the system. The physical explanation for the latter is that

<sup>2</sup>Note in particular that the performance requirement for the levels are very lax, as the allowed error is much larger than the allowed setpoint change. This is reasonable since we have no strict requirements for level control, but rather want to use variations in level to avoid sudden changes in the product flows,  $D$  and  $B$ .

<sup>3</sup>Recall that we assume that the heat duties  $Q_C$  and  $Q_R$  may be manipulated directly. If self regulation is included the negative RGA-element will most likely disappear.

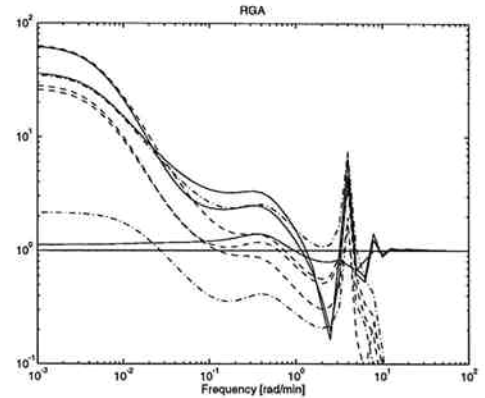


Fig. 3: Relative Gain Array elements as function of frequency (solid lines: diagonal elements).

manipulation of  $D$  affects  $M_D$ , and  $B$  affects  $M_B$ , but has almost no influence on the other outputs. Thus, one of the main advantage with the LV-configuration is that composition control is insensitive to the tuning of the level loops.

The  $3 \times 3$  interaction for the composition and pressure subsystem could in principle be corrected for by a multivariable controller, for example a decoupler. However, the large RGA elements signal high sensitivity to diagonal input uncertainty (e.g., Skogestad and Morari, 1987) and thereby prevent the use of a decoupler. Thus, we may already at this stage conclude that it is essential to consider input uncertainty when tuning a multivariable controller.

**RHP-zeros.** The model has no multivariable right half plane (RHP) zeros. However, there are RHP zeros in several elements, as shown from the inverse responses in Fig.2. Specifically, a change in cooling duty  $Q_c$  yields an inverse response for all outputs, except for the pressure. The main reason behind this is that a change in  $Q_c$  yields an inverse response for the vapor flow  $V_T$  entering the condenser: Initially, an increase in cooling yield a fast increase in  $V_T$ . However, because pressure starts decreasing, the column temperature also decreases, and the heat of vaporization increases leading to a decrease in  $V_T = Q_c / H^{vap}$ . The inverse responses are very slow (zero location  $z_{13} = 0.0367; z_{23} = 0.0264; z_{43} = 0.0204; z_{53} = 0.0580 \text{ min}^{-1}$ ), so for single-loop control the cooling duty should be used to control pressure, that is, pairing on a negative RGA-element. Since there is no RHP zero for the pressure (3,3-element) and since the  $5 \times 5$  system has no RHP transmission zeros, the negative RGA (3,3-element) must imply that there is a RHP transmission zero in the remaining subsystem (Hovd and Skogestad, 1992). Indeed, we find that the upper  $2 \times 2$  system (from  $L_T$  and  $Q_R$  to  $x_D$  and  $x_B$ ) has a RHP transmission zero at  $0.0129 \text{ min}^{-1}$  (the lower  $2 \times 2$  system is decoupled and does not influence this value). This RHP zero may cause instability if the pressure control fails when using decentralized control (see below).

**Input saturation.** Input saturation imposes a fun-

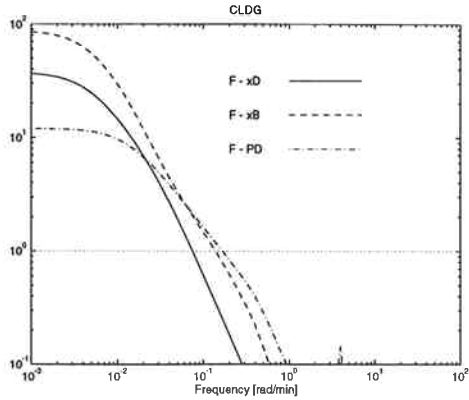


Fig. 4: Closed Loop Disturbance Gain for decentralized control.

damental limitation on the control performance. The inputs required for perfect control are  $u = G^{-1}r + G^{-1}G_d d$ . Thus, in terms of scaled variables the elements in the matrices  $G^{-1}$  and  $G^{-1}G_d$  should be less than 1 in the frequency range where control is needed. For our example, with the allowed variations in the inputs as given by  $u_{max}$  in Table 2, we find from frequency-dependent plots of the elements of these matrices (not shown) that input saturation is not a serious problem, even at relatively high frequencies.

**Decentralized control.** From the frequency-dependent RGA-plot in Fig.3 we note that the diagonal elements are fairly large (about 3) also in the frequency-region important for control. Thus, we can expect interactions at high frequencies. To evaluate performance for setpoint changes the Performance RGA, which is scaling dependent, is the appropriate tool. This is not shown here, but one main finding is that the worst setpoint change is for top composition,  $x_{D,s}$ , and in particular that a strong interaction is expected for the pressure.

The closed-loop disturbance gains (CLDG) yield the effect of disturbances under decentralized control. For all outputs the worst disturbance is the feed rate  $F$ , and the effect of this disturbance is given in Fig.4. The bandwidth requirement for rejecting a 15% disturbance in  $F$  is about 14 min for top composition ( $x_D$ ), 7 min for bottom composition ( $x_B$ ) and 6 min for top pressure ( $P_D$ ).

The controllability analysis for decentralized control indicates that  $x_{D,s}$  is the most difficult setpoint to track and  $F$  is the most difficult disturbance to reject (for this system and with the scalings used here). This has also been confirmed by simulations. All simulations presented in the paper will therefore show responses to changes of  $x_{D,s}$  (+0.01 i.e. +1 in scaled variables, and  $F$  (+30%).

The conclusion from the controllability analysis is that decentralized control is difficult for this system, and this is confirmed from the simulations in Fig.5. The pressure control loop has a time constant of 3 min, and the composition loops of about 15 min. (individually,

i.e., without considering interactions). The level loops, which have essentially no effect of the rest of the system, were very loosely tuned (30 min).

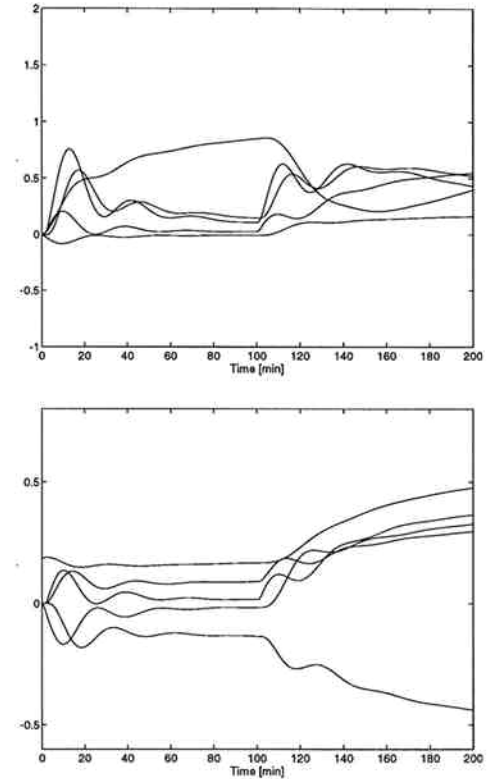


Fig. 5: Simulated decentralized control performance for change in setpoint for  $x_D$  at  $t = 0$  and 30% feed disturbance at  $t = 100$  min. Upper plot: Outputs. Lower plot: Inputs.

#### 4 $\mathcal{H}_\infty/\mu$ control

In this section we study the *unconstrained* control problem using the  $\mathcal{H}_\infty/\mu$  framework. The  $\mathcal{H}_\infty$ -norm is used because it is rather straightforward to specify the desired responses in terms of ‘classical’ measures such as closed-loop time constants, allowable steady state offset and acceptable overshoot. For readers who are not familiar with the  $\mathcal{H}_\infty$ -norm it suffices to say that it is an upper bound on the frequency magnitude of the closed-loop transfer function. As is seen in this paper the results using this norm are often not too different from the conventional quadratic performance criterion (denoted the  $\mathcal{H}_2$ -norm in mathematical terms) for the output, but the weights for the problem (the ‘knobs’ or tuning parameters) may have to be somewhat changed. However, one significant advantage with the  $\mathcal{H}_\infty$ -norm is that it allows worst-case model uncertainty to be included explicitly (using the structured singular value, denoted SSV or  $\mu$ ).

The block diagram in Fig.6 defines the problem studied in this section.  $K$  is the controller to be designed. It may be a two-degree-of-freedom (TDF)

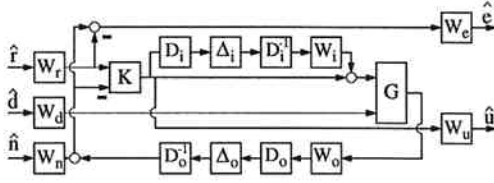


Fig. 6: Block diagram for robust  $\mathcal{H}_\infty$ -problem.

controller with separated inputs  $r$  (setpoint) and  $y_m$  (measured outputs) as in the figure, or with a one-degree-of-freedom controller (ODF) with input  $r - y_m$ .

$G$  is the normalized (scaled) plant model with 8 inputs (5 manipulated inputs  $u$  and 3 unmeasured disturbances  $d$ ) and 5 outputs  $y$ . The scalings are given in Table 2.  $W_r$ ,  $W_d$  and  $W_n$  are weight matrices for setpoints  $r$ , disturbances  $d$  and measurement noise  $n$ , respectively.  $W_e$  and  $W_u$  are weights on deviation from desired setpoint,  $e$ , and manipulated inputs  $u$ , respectively. The weighting matrices are diagonal with elements  $[W_r] = r_{max}/y_{max}$ ,  $[W_d] = 1$ ,  $[W_n] = 0.01$ ,  $[W_u] = 1$  and

$$[W_e](s) = \frac{1}{M} \frac{\tau_{cl}s + M}{\tau_{cl}s + A}; \quad M = 2, A = 0.0001 \quad (1)$$

with  $\tau_{cl} = [30 \ 30 \ 30 \ 60 \ 60]$  min. For the compositions, for which the setpoints  $r$  and controlled outputs  $y$  have identical scalings,  $M$  is the maximum allowed peak of the sensitivity function and  $\tau_{cl}$  is the required closed-loop response time for that output. Note that  $A$  is very small so that integral action is in practice required for all outputs.

The model uncertainty is also represented within the  $\mathcal{H}_\infty$ -framework, that is,  $\Delta_i$  and  $\Delta_o$  are any diagonal matrices with  $\mathcal{H}_\infty$ -norm less than one. 10% relative input gain uncertainty is allowed in each input, that is,  $W_i = 0.1 * I_5$ . The output uncertainty has the form  $w_o(s) = \frac{\theta s}{(\theta/2)s + 1}$  which allows for a delay of approximately  $\theta = 1$  min in each measurement.

We arrived at this problem formulation and these weight through several steps, starting with a pure  $\mathcal{H}_\infty$ -problem with only setpoints and no uncertainty and ending up with the overall  $\mu$ -problem as defined by Fig.6. We shall go through some of these steps because it yields some insight.

**Setpoint tracking with no uncertainty.** This corresponds to the case with  $\hat{d} = 0$ ,  $\Delta_i = 0$ ,  $\Delta_o = 0$  and yields a pure  $\mathcal{H}_\infty$ -problem for which synthesis software is readily available (Balas et.al 1991, Chiang and Safonov, 1992). The optimal controller yields a closed-loop  $\mathcal{H}_\infty$ -norm equal to 0.83. Since this is less than 1 the performance requirement for the worst case direction is achieved with some margin. The obtained controller uses rather high gains at high frequencies; the ‘roll-off’ frequency is about 10 [rad/min]. This is typical for all the cases we studied and it may be avoided using a slightly sub-optimal controller with higher  $\mathcal{H}_\infty$ -norm. This sub-optimal controller yields 1) a blend of  $\mathcal{H}_\infty$  and  $\mathcal{H}_2$  optimality (which is desirable since our ultimate objective is

to use model predictive control which uses the  $\mathcal{H}_2$ -norm), and 2) a ‘roll-off’ at lower frequency resulting in better robustness with respect to high frequency uncertainty. For this case a sub-optimal controller with  $\mathcal{H}_\infty$ -norm equal to 1.0 (rather than 0.83) gave approximately the same low-frequency behavior as the optimal controller, but a ‘roll-off’ frequency of about 0.2 [rad/min].

The obtained controller is a ‘full’  $5 \times 5$  controller, however, a more careful analysis of the controller reveals the following two interesting properties: 1) The controller may be decomposed into a  $3 \times 3$  controller and two single-loop controllers for the levels, corresponding to a multivariable LV-configuration. 2) The remaining  $3 \times 3$  controller is essentially a decoupler. This may be seen by evaluating the condition number of  $GK$ . These two statements are *not* true when disturbances and/or uncertainty is considered, as discussed below.

**Including model uncertainty.** To analyze a system with model uncertainty we ‘pull out’ the  $\Delta$ -blocks from the block diagram and get instead of the block diagram in Fig.6 a  $M \Delta$ -structure where  $M$  contains some additional inputs and outputs representing the ‘disturbances’ caused by the uncertainty. To analyze such a system we must use the structured singular value,  $\mu$ , instead of the  $\mathcal{H}_\infty$ -norm. In this paper we use as a tight approximation for  $\mu$  the scaled  $\mathcal{H}_\infty$ -norm,  $\min_D \|DM D^{-1}\|_\infty$ . The structure of the  $D$ -scales depend on the model uncertainty. In our case with diagonal uncertainty at the input and the output we get  $D = \text{diag}\{D_i, D_o, I_5\}$  where  $D_i$  and  $D_o$  are diagonal matrices each with 5 parameters (which are ‘adjusted’ to represent the worst-case uncertainty). The  $\mu$ -optimal controller is then obtained by  $D - K$ -iteration (Doyle, 1983). Usually one only does a few iterations such that a sub-optimal  $\mu$ -controller is obtained.

**Setpoint tracking with input uncertainty.** To consider the effect of model uncertainty we added input uncertainty (i.e., no disturbances or output uncertainty) and obtained an optimal controller by  $DK$ -iteration. We found that this  $\mathcal{H}_\infty$  controller can be reasonably well approximated by a decentralized L/D V/B - configuration (compare with Eq.11 in Skogestad and Morari, 1987). In this scheme  $D$  is computed from  $M_D$ ,  $B$  is computed from  $M_B$ , but  $L_T$  is computed from both  $x_D$  and  $M_D$  and  $V$  is computed from both  $x_B$  and  $M_B$ . These results are consistent with earlier findings which found that this configuration has much lower RGA-values and is preferable when there is input uncertainty.

**With disturbances and input uncertainty.** The results in this case with respect to the controller structure are qualitatively the same as found above, and the  $\mu$ -value for the overall problem was about 1.2. The response of this controller is shown by the dotted lines in Fig.7.

**Final remarks.** Some final remarks seem in order. Most of these are in accordance with previous

findings.

1) With the scalings used for the plant, the optimal input uncertainty  $D$ -scales are close to 1 for all cases. The optimal  $D$ -scales for the output uncertainty are about 5.

2) The weights were chosen to yield  $\mu \approx 1 \pm 0.2$  for all problems. The reason is that interpretation of  $\mu$  is difficult if it is too different from 1.

3) A controller designed for setpoint changes only, does not perform well if disturbances are considered.

4) A controller designed without considering input uncertainty performs poorly with input uncertainty.

5) A controller designed without considering output uncertainty performs well if the controller is slightly  $\mathcal{H}_\infty$  sub optimal.

## 5 Model Predictive $5 \times 5$ control

In this section we use a Model Predictive Control algorithm which involves constrained on-line optimization over a finite receding horizon to explicitly address input constraints. There are numerous implementations of these schemes, and they differ mainly in the way future outputs are predicted. The commonly used DMC implementation makes the crude assumption that all disturbances act as steps on the outputs, but as shown by Lundström et al. (1991) this may lead to poor results when both compositions are controlled. Therefore, we use a state observer with the steady state Kalman filter gain<sup>4</sup>. The tuning parameters for this MPC controller are:  $H_p$  the output prediction horizon,  $H_c$  the control horizon,  $\Lambda_y$  output weight,  $\Lambda_u$  input weight and  $K_f$  the Kalman filter gain. The filter gain is a function of the disturbance model and the disturbance and noise covariance matrices.

Recently Lee and Yo (1994) presented tuning rules for obtaining robust MPC performance. For the case of diagonal input uncertainty they penalize the input moves using  $\Lambda_u$  in order to obtain robustness. Applying this method to the distillation problem from Skogestad et al (1988) gave  $\mu_{RP} = 2.23$ , whereas the optimal value is known to be less than 0.978 (Lundström et. al (1991). This is not satisfactory, therefore, in this paper we use the observer parameters to obtain robustness with respect to input uncertainty.

Our main objective is to use the weights obtained from the rigorous robustness analysis in the previous section as a starting points for weight selection for the MPC controller. There are several difficulties here. First, the MPC scheme uses the  $\mathcal{H}_2$ -norm rather than the  $\mathcal{H}_\infty$ -norm. Second, the MPC controller is a finite horizon controller which contains additional tuning parameters. Third, uncertainty can not be included explicitly. In spite of these difficulties, we were able to tune the MPC controller to mimic the  $\mu$ -controller very closely. The final tuning of the response time was

<sup>4</sup>The MPC controller we use here is from the program "scmpc" in the the MPC-toolbox for MATLAB (Morari et al. 1991) and is due to Ricker and coworkers at the University of Washington.

done by adjusting a single parameter  $\alpha$  in the output weight to minimize  $\mu$  in the robustness problem defined in the previous section. The input uncertainty was represented as disturbances, while output uncertainty was not included since the robustness analysis found that this uncertainty was not crucial. The tuning parameters are summarized next.

*Optimization part of MPC controller.* Sampling time: 1 min, horizons  $H_p = 60$  and  $H_c = 3$ .

$$\Lambda_y = \alpha W_e; \quad \Lambda_u = |W_u| + |W_i D_i| \quad (2)$$

(where  $W_e$  and  $W_u$  are the  $\mathcal{H}_\infty$ -weights and  $D_i$  the  $D$ -scale representing the input uncertainty).

*Kalman filter part of MPC controller.* Augmented disturbance model to include model uncertainty

$$G_d = C(sI - A)^{-1}B = G \text{diag}\{W_i D_i^{-1}, W_d\} \quad (3)$$

This leads to the Kalman filter gain  $K_f = P_f C^T V^{-1}$  where  $P_f$  is obtained by solving the Riccati equation  $P_f A^T + A P_f - P_f C^T V^{-1} C P_f + B W B^T = 0$  where the covariance matrices for disturbance is  $W = I_8$  and for noise is  $V = W_n^2$ .

For each value of  $\alpha$  we obtained the frequency response of the discrete controller and added hold elements at the inputs and outputs to the controller. Using the same problem specification as in the previous section we minimized  $\mu$  and obtained a value  $\mu = 1.15$  for  $\alpha = 0.03$ . The linear robust performance was thus in fact somewhat better than the sub-optimal controller obtained by  $DK$ -iteration.

The solid lines in Fig.7 show the simulated performance of the MPC controller when no constraints are active, that is, when it behaves like a linear controller. The response is seen to be very similar to the  $\mu$ -optimal controller found previously (dotted lines). The main difference is the speed of response of the levels and the use of inputs  $D$  and  $B$ .

In Fig.8 is shown the MPC responses when  $Q_C$  is constrained to be at its nominal value. As we see, the MPC controller preserves stability, and manages to keep the levels and the pressure close to their desired values. However, the composition control is relatively poor since these can not be maintained at their setpoints when one degree of freedom is lost.

### Some final remarks.

1. In the simulations we used a 1 minute delay in each measurement and used -20% input gain error in all inputs except  $Q_R$  which has +20% uncertainty.<sup>5</sup>

2. The unconstrained simulation shows that the controller performs well both for setpoint tracking and disturbance rejection. No excessive input usage is required. The performance for the outputs in Fig.7 is significantly better than for the decentralized scheme shown in Fig.5.

3. In the constrained case the use of a MPC scheme avoids the need for complicated logics including overrides and retuning. If the decentralized control scheme from Section 3 is used, then the system goes unstable when  $Q_C$  is fixed. The multivariable  $\mu$ -controller does

<sup>5</sup>This input uncertainty was found to be the worst of all  $\pm 20\%$  combinations.

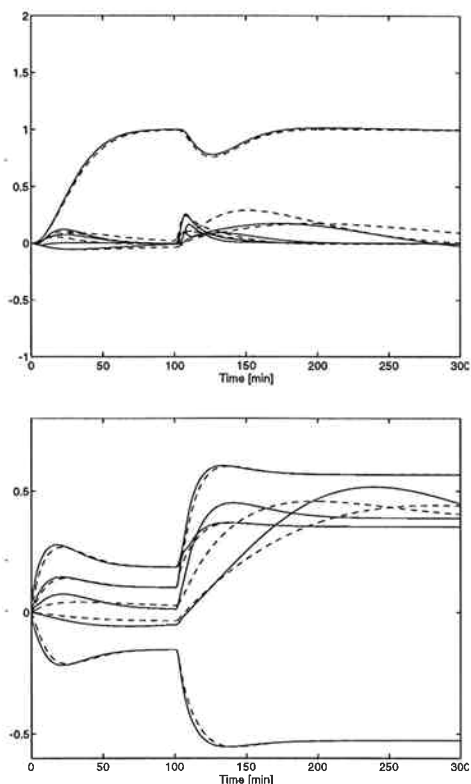


Fig. 7: Simulated unconstrained control performance. Solid lines: MPC. Dotted lines:  $\mu$ -controller

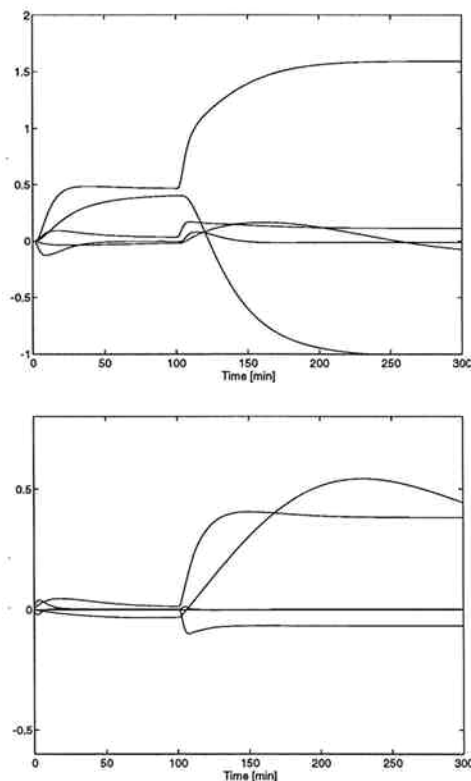


Fig. 8: Simulated MPC performance with  $Q_C$  constant.

not go unstable, but performs very poorly, and simulations show that it goes unstable when  $Q_R$  is fixed.

## 6 Conclusions

The results in this paper indicates that the main advantages with  $5 \times 5$  distillation control are improved disturbance detection by indirect use of the level and pressure measurements, and explicit input constraint handling. One difficulty is the tuning of the controller, but in our example we were able to tune the MPC scheme quite easily to get acceptable robustness. The following procedure was used: 1) Define a robust  $\mathcal{H}_\infty$ -problem with an optimal  $\mu$ -value close to 1. 2) Use the weights and scaling found for this problem to derive MPC tuning parameters. The critical uncertainty, in this case at the inputs, is represented as fictitious disturbances. 3) One adjustable parameter in the MPC controller is used to minimize  $\mu$ . 4) Time simulations are used to check the results and possible adjust some weights. The resulting controller is not 'optimal' in any mathematical sense, but was found to perform very well.

## References

- Balas, G.J., Doyle, J.C., Glover, K., Packard, A. and Smith, R., 1991, " $\mu$ -Analysis and Synthesis Toolbox", The Mathworks, Inc.
- Bennett, D.L., Agrawal, R. and Cook, P.J. (1983), "New pressure drop correlations for sieve tray distillation columns", *AIChE Journal*, **29**, 3, 434-442.
- Chiang, R.Y. and Safonov, M.G., 1992, "Robust Control Toolbox", The Mathworks, Inc.
- Doyle, J.C., 1982, "Analysis of feedback systems with structured uncertainties", *IEEE Proc. Part D*, **129**, 242-250.
- Doyle, J.C., 1983, "Synthesis of robust controllers and filters", *Proc. IEEE Conf. Decision Contr.*, San Antonio, TX.
- Grosdidier, P., Morari, M. and Holt, B.R., 1985, "Closed-Loop Properties from Steady-State Gain Information", *Ind. Eng. Chem. Fundam.*, **24**, 221-235.
- Hovd, M. and Skogestad, S., 1992, "Simple frequency-dependent tools for control system analysis, structure selection and design", *Automatica*, **28**, 989-996.
- Lee, J.H. and Yu, Z.H., "Tuning of model predictive controllers for robust performance", *Comp.Chem.Engng.*, **18**, 15-37.
- Rademaker, O., Rijnsdorp, J.E. and Maarleveld, A., 1975, "Dynamics and control of continuous distillation units", Elsevier, Amsterdam.
- Skogestad, S. and Morari, M., 1987, "Control configuration selection for distillation columns", *AIChE Journal*, **33**, 1620-1635.
- Skogestad, S. and Morari, M., 1988, "Understanding the dynamic behavior of distillation columns", *Ind. Eng. Chem. Res.*, **27**, 10, 1848-1862.
- Wolff, E.A., Skogestad, S., Hovd, M. and Mathisen, K.W., 1992, "A procedure for controllability analysis", *Preprints IFAC workshop on Interactions between process design and process control*, London, Sept. 1992, J. Perkins (Ed.), Pergamon Press, 123-132.